Inorg. Chem. **2008**, *47*, 3135−3139

Formation of Indium Nitride Nanorods within Mesoporous Silica SBA-15

Shih-Chieh Chang and Michael H. Huang*

Department of Chemistry, National Tsing Hua University, Hsinchu 30013, Taiwan

Received November 1, 2007

We report the first formation of arrays of InN nanorods inside the nanoscale channels of mesoporous silica SBA-15. $In(NO_3)_3$ dissolved in methanol was incorporated into SBA-15 powder without prior pore surface functionalization. Formation of InN nanorod arrays was carried out by ammonolysis at 700 °C for 8 h. The final products have been characterized by FT-IR spectra, ^{29}Si MAS NMR spectra, Raman spectra, XRD patterns, TEM images, nitrogen adsorption–desorption isotherm measurements, and optical spectroscopy. The freestanding InN nanorods observed after silica framework removal with HF solution show diameters of 6–7.5 nm and lengths of 25–50 nm. Formation of a trace amount of In_2O_3 was also verified. The InN nanorods exhibit a broad band centered at around 550–600 nm, and a band gap energy of 1.5 eV was determined. No light absorption in the near-IR region was measured. The nanorods give a weak emission band centered at around 600 nm. These optical properties are believed to be related to the possible incorporation of oxygen during InN nanorod synthesis.

Introduction

Studies on the preparation of indium nitride (InN) nanostructures have begun to receive greater attention in recent years. InN has promising optical properties and a large electron drift velocity at room temperature, making it potentially useful for applications in high-speed field-effect transistors and optoelectronic devices.[1,2] The band gap energy of InN was recently found to be between 0.7 and 0.8 eV, much lower than the previously believed value of 1.9 eV.[3] The optical band gap can vary continuously from ∼0.7 to 2 eV, depending on the free electron concentrations of the synthesized InN materials.[4] Incorporation of a few percent of oxygen in polycrystalline InN can widen the band gap to over 2.2 eV.[5] Among the approaches used to make InN nanostructures, the thermal chemical vapor transport and deposition method under an ammonia flow has been widely used to grow micron-sized nanowires and nanorods on substrates.[6–11] Solvothermal approaches have been adopted to grow quasi-spherical InN nanoparticles at relatively low temperatures of 300 °C or less to avoid their thermal decomposition.[12–14] Different indium and nitrogen source reagents were used in these studies, and the particle sizes are mostly in the range of 10–30 nm in diameter. A solution−liquid–solid mechanism has also been used to grow InN fibers of 100–1000 nm in length from azido−indium precursors at 203 °C.[15] Despite these efforts, the controlled growth of relatively uniform InN nanorods with diameters of a few nanometers and lengths of tens of nanometers still has not been achieved. Mesoporous silica SBA-15 possesses

(1) Bhuiyan, A. G.; Hashimoto, A.; Yamamoto, A. *J. Appl. Phys.* **2003**, *94*, 2779.
(2) O'Leary, S. K.; Foutz, B. E.; Shur, M. S.; Bhapkar, U. V.; Eastman, L. F. *J. Appl. Phys.* **1998**, *83*, 826.
(3) Wu, J.; Haller, E. E.; Lu, H.; Schaff, W. J.; Saito, Y.; Nanishi, Y. *Appl. Phys. Lett.* **2002**, *80*, 3967.
(4) Wu, J.; Walukiewicz, W.; Li, S. X.; Armitage, R.; Ho, J. C.; Weber, E. R.; Haller, E. E.; Lu, H.; Schaff, W. J.; Barcz, A.; Jakiela, R. *Appl. Phys. Lett.* **2004**, *84*, 2805.
(5) Yoshimoto, M.; Yamamoto, H.; Huang, W.; Harima, H.; Saraie, J.; Chayahara, A.; Horino, Y. *Appl. Phys. Lett.* **2003**, *83*, 3480.
(6) Vaddiraju, S.; Mohite, A.; Chin, A.; Meyyappan, M.; Sumanasekera, G.; Alphenaar, B. W.; Sunkara, M. K. *Nano Lett.* **2005**, *5*, 1625.
(7) Hu, M.-S.; Wang, W.-M.; Chen, T. T.; Hong, L.-S.; Chen, C.-W.; Chen, C.-C.; Chen, Y.-F.; Chen, K.-H.; Chen, L.-C. *Adv. Funct. Mater.* **2006**, *16*, 537.
(8) Luo, S.; Zhou, W.; Zhang, Z.; Liu, L.; Dou, X.; Wang, J.; Zhao, X.; Liu, D.; Gao, Y.; Song, L.; Xiang, Y.; Zhou, J.; Xie, S. *Small* **2005**, *1*, 1004.
(9) Johnson, M. C.; Lee, C. J.; Bourret-Courchesne, E. D.; Konsek, S. L.; Aloni, S.; Han, W. Q.; Zettl, A. *Appl. Phys. Lett.* **2004**, *85*, 5670.
(10) Lan, Z. H.; Wang, W. M.; Sun, C. L.; Shi, S. C.; Hsu, C. W.; Chen, T. T.; Chen, K. H.; Chen, C. C.; Chen, Y. F.; Chen, L. C. *J. Cryst. Growth* **2004**, *269*, 87.
(11) Kryliouk, O.; Park, H. J.; Won, Y. S.; Anderson, T.; Davydov, A.; Levin, I.; Kim, J. H.; Freitas, J. A., Jr. *Nanotechnology* **2007**, *18*, 135606.
(12) (a) Sardar, K.; Deepak, F. L.; Govindaraj, A.; Seikh, M. M.; Rao, C. N. R. *Small* **2005**, *1*, 91. (b) Sardar, K.; Dan, M.; Schwenzer, B.; Rao, C. N. R. *J. Mater. Chem.* **2005**, *15*, 2175.
(13) Xiao, J.; Xie, Y.; Tang, R.; Luo, W. *Inorg. Chem.* **2003**, *42*, 107.
(14) Wu, C.; Li, T.; Lei, L.; Hu, S.; Liu, Y.; Xie, Y. *New J. Chem.* **2005**, *29*, 1610.

10.1021/ic702155w CCC: $40.75
Published on Web 03/01/2008

hexagonally arranged pore channels of a few nanometers in diameter and serves as a suitable candidate for the confined growth of rodlike InN nanostructures. Our previous work has demonstrated the successful formation of TiN nanoparticles and arrays of GaN nanorods within the pore channels of SBA-15.[16,17] These studies showed that mesoporous silica materials can serve as effective templates for the growth of elongated and size-controlled nitride nanostructures, which are typically difficult to make using other synthetic routes.

Here we describe the extensive formation of short InN nanorods within the pore channels of SBA-15 powder via a convenient infiltration method without pore surface functionalization with methyl groups as previously used. $In(NO_3)_3$ dissolved in methanol was introduced into the interior of SBA-15. Subsequent ammonolysis at an appropriate temperature generated crystalline InN nanorods. The products have been characterized with several spectroscopic techniques and electron microscopy. The optical properties of these InN nanorods were also examined.

Experimental Section

Mesoporous silica SBA-15 was synthesized by following our previously described procedure with slight modifications.[17] First, 2.0 g of triblock copolymer Pluronic P-123 surfactant (Aldrich) was added to a solution containing 15 g of deionized water and 60 g of 2 M HCl at 40 °C with stirring until the copolymer completely dissolved. Then 4.25 g of tetraethyl orthosilicate (TEOS, Acros Organics) was added and the mixture stirred for 12 h at 40 °C. The mixture was transferred to a sealed container and heated to 100 °C in an oven for 20 h. The resulting white precipitate was filtered, washed with water and ethanol, and dried at 65 °C overnight. Finally, the copolymer was removed by calcination in air at 550 °C for 3 h.

Next, 0.5 g of $In(NO_3)_3 \cdot xH_2O$ (Aldrich, 99.99%) was added to 3 mL of methanol and the mixture stirred until dissolved. The mixture was added drop-by-drop to a 100 mL round-bottom flask containing 0.1 g of SBA-15 powder. After the mixture was stirred for 24 h, the powder was filtered, washed with 1 mL of methanol, and dried at 65 °C overnight. The precursor-impregnated SBA-15 powder was placed in a ceramic boat, which was inserted into the center of a 1 in. quartz tube in a tube furnace. The quartz tube was purged with ammonia flow at 90 sccm for 90 min. No vacuum pump was used to control the quartz tube pressure. After that, the furnace temperature was increased to 700 °C over 20 min and held at 700 °C for 8 h. Lower reaction temperatures cannot be used because the product was found to be mainly In_2O_3; thermal decomposition of InN appears to be prevented at 700 °C in this system. At the end of this process, the furnace was rapidly cooled to room temperature. During cooling, the ammonia flow continued to prevent possible thermal decomposition of InN. Brown products were obtained.

The Fourier transform infrared spectrum (FT-IR) of calcined SBA-15 powder was recorded on a Perkin-Elmer Spectrum RX I spectrometer. The solid-state ^{29}Si magic-angle spinning nuclear magnetic resonance (MAS NMR) spectrum of calcined SBA-15 was recorded on a Bruker DSX400WB spectrometer. Low-angle and high-angle X-ray diffraction (XRD) patterns were obtained using MAC Science MXP-18 and Shimadzu XRD-6000 diffractometers, respectively, with Cu Kα radiation. Transmission electron microscopy (TEM) images were taken using JEOL JEM-1200CX, JEM-2010, and JEM-3000F transmission electron microscopes. TEM samples of InN nanorods incorporated within SBA-15 were prepared by ultramicrotoming an SBA-15/epoxy mixture to thin slices of approximately 50 nm in thickness. To perform TEM characterization of freestanding InN nanorods, SBA-15 powder was added to an amorphous carbon-coated TEM grid and treated with a drop of 40% HF solution to remove the silica framework. Nitrogen adsorption–desorption isotherms were measured at 77 K using a Quantachrome Nova2000e analyzer. A micro-Raman spectroscopy system was employed to acquire Raman spectra of the InN nanorods with an excitation wavelength of 632.8 nm from a He−Ne laser. Diffuse reflectance spectra of InN-incorporated SBA-15 powder in the range of 240–800 nm were recorded on a Hitachi U-3310 spectrophotometer equipped with an integrating sphere. For absorption spectra of the InN sample in the near-infrared (near-IR) region, a JASCO V-570 spectrophotometer was used. After the silica template was removed with 2.0 M NaOH and centrifugation was carried out at 8000 rpm for 30 min, InN nanorods dispersed in deionized water were added to a microscope glass and dried for spectral measurement. A He−Cd laser with an excitation wavelength of 325 nm and a Si-based detector was used to take photoluminescence spectra.

Results and Discussion

The calcined SBA-15 powder was characterized with FT-IR spectroscopy, which reveals the expected strong peaks from the Si−O−Si stretching vibrations and the O−H stretching vibrations of the silanol groups (see the Supporting Information). ^{29}Si MAS NMR spectrum further indicates a highly condensed framework structure with a strong Q^4 signal and weaker Q^3 and Q^2 peaks (see the Supporting Information). This silicate structure may lead to a decrease in the polarity of the pore surfaces. In this study, $In(NO_3)_3$ was dissolved in methanol and introduced into the interior of SBA-15. Methanol, which has a dielectric constant lower than that of water ($\epsilon = 33$ vs 78), is a suitable medium for loading indium nitrate into the hydrophilic pore channels with a lower polarity. In addition, the lower surface tension of methanol (22.61 dynes/cm at 20 °C) than that of water (73.05 dynes/cm at 18 °C) allows it to more easily soak into the mesopores.[18] Ethanol was not used because of the solubility problem with $In(NO_3)_3$. Thus, by an appropriate choice of indium precursor and solvent, pore surface functionalization with methyl groups was not needed.

The structure of mesoporous silica SBA-15 and the formation of InN nanostructures were characterized by XRD patterns. Figure 1 shows the low-angle XRD patterns of calcined SBA-15 and InN-incorporated SBA-15. The diffraction patterns indicate that the framework still possesses a long-range ordered hexagonal structure after the formation of InN nanostructures. The (100) peak is shifted to 1.08° 2θ, corresponding to a d spacing of 81.8 Å (from 92.0 Å for calcined SBA-15), possibly due to a higher degree of

(15) Dingman, S. D.; Rath, N. P.; Markowitz, P. D.; Gibbons, P. C.; Buhro, W. E. *Angew. Chem., Int. Ed.* **2000**, *39*, 1470.
(16) Hsueh, H.-S.; Yang, C.-T.; Zink, J. I.; Huang, M. H. *J. Phys. Chem. B* **2005**, *109*, 4404.
(17) Yang, C.-T.; Huang, M. H. *J. Phys. Chem. B* **2005**, *109*, 17842.
(18) Weast, R. C. *Handbook of Chemistry and Physics*, 52nd ed.; CRC Publishing: Boca Raton, FL, 1971; p F-32.

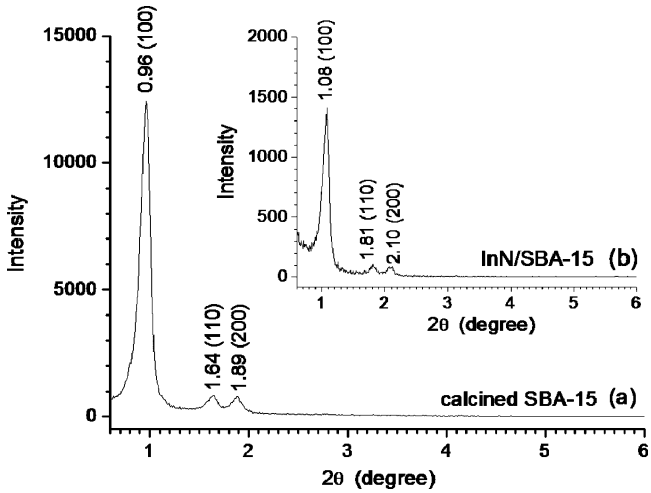

Figure 1. Low-angle XRD patterns of (a) calcined SBA-15 and (b) InN-incorporated SBA-15.

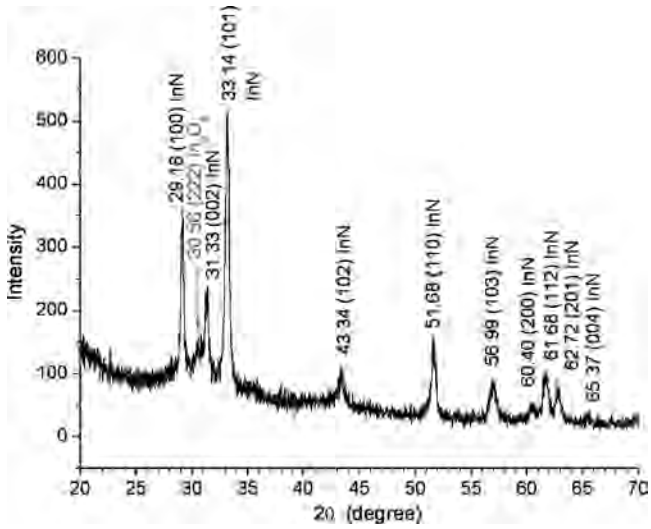

Figure 2. XRD pattern of the InN nanostructures formed within SBA-15.

silicate condensation after the heat treatment to form the InN nanostructures. Figure 2 gives the high-angle XRD pattern of InN-incorporated SBA-15. This diffraction pattern matches well with that of wurtzite InN (JCPDF No. 50-1239), confirming the successful formation of InN nanostructures. A weak peak attributed to In_2O_3 was also recorded, suggesting the formation of a trace amount of body-centered cubic indium oxide. This result is reasonable, as ammonolysis at 650 °C was found to produce largely In_2O_3 nanostructures (data not shown). Raman spectrum of the InN-incorporated SBA-15 is displayed in Figure 3. The peaks at 453, 490, and 570 cm^{-1} can be assigned to the A_1 transverse optical (TO) and E_2 and A_1 longitudinal optical (LO) phonon modes of hexagonal InN, respectively.[10]

Direct evidence of the formation of InN nanorods within mesoporous silica SBA-15 was obtained by TEM characterization. Figure 4 is a low-magnification TEM image of SBA-15 powder loaded with rodlike InN nanostructures. Extensive arrays of the InN nanostructures were formed and followed the curvature of the pore channels over long distances. Almost no InN nanoparticles can be found outside

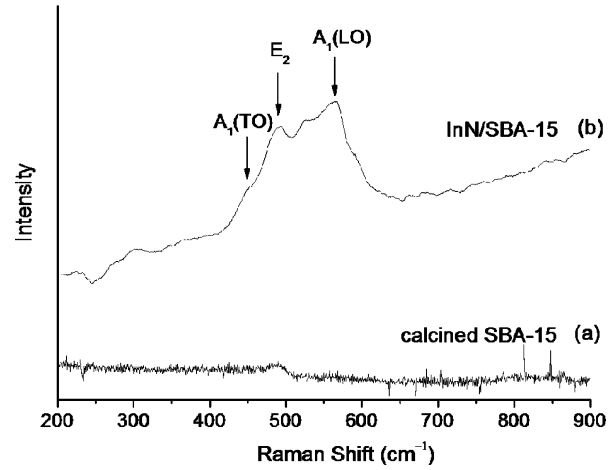

Figure 3. Raman spectra of (a) calcined SBA-15 and (b) InN-incorporated SBA-15. The peak at 523 cm^{-1} is the signal from the silicon substrate.

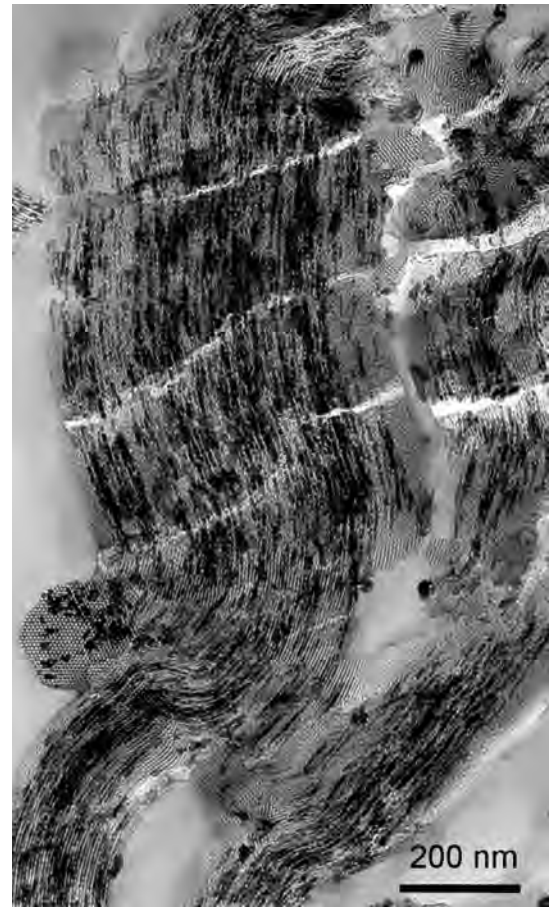

Figure 4. Low-magnification TEM image of an ultramicrotomed InN-incorporated SBA-15 sample.

the channels. Figure 5 provides a TEM image of the freestanding InN nanorods after silica removal with HF solution. Relatively uniform nanorods with lengths of primarily 25–50 nm and diameters of 6–7.5 nm are densely dispersed on the TEM grid. Notice that the nanorods do not possess smooth surfaces, and their diameters can be slightly larger than those of the pore channels. Some of these nanorods show side-by-side arrangement because there are connecting points between adjacent rods, in addition to the reason of their close relative positions before silica removal.

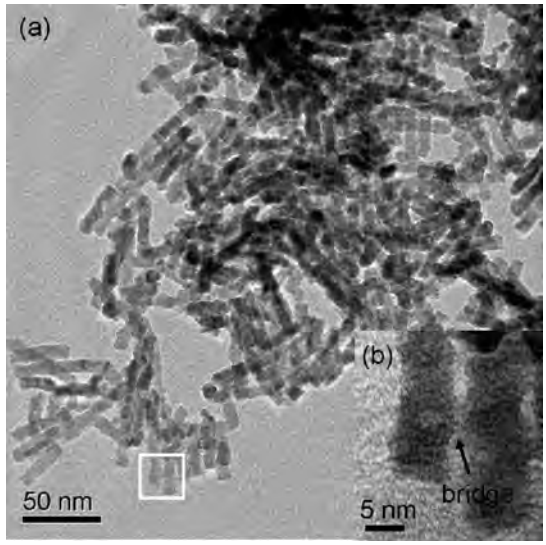

Figure 5. (a) TEM image of the free-standing InN nanorods. (b) High-magnification TEM image of the square region in (a) showing the bridge between adjacent nanorods.

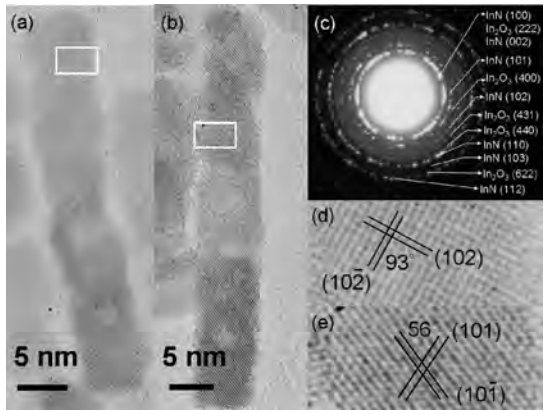

Figure 6. (a, b) High-resolution TEM images of individual InN nanorods. (c) SAED pattern of the free-standing InN nanorods. (d, e) Close views of the rectangular regions in (a) and (b), respectively, showing clear lattice fringes.

These findings suggest the formation of InN nanorods in the micropore regions on the silica walls. SBA-15 possesses additional micropores because of the templating agent Pluronic P-123 used; the hydrophilic ethylene oxide chains can penetrate into the silica walls during the synthesis.[19] High-resolution TEM images of individual InN nanorods are shown in Figure 6. In one nanorod, two sets of lattice fringes at an angle of 93° can be clearly discerned with the same *d* spacing of 2.08 Å (Figures 6a,d). These lattice fringes correspond to the (102) and (10$\bar{2}$) planes of hexagonal InN. Another nanorod also exhibits two sets of well-resolved lattice fringes at an angle of 56° with the same *d* spacing of 2.68 Å, which should correspond to the (101) and (10$\bar{1}$) planes of InN. These angles are in accord with those determined by using the CaRIne Crystallography program. Some of these nanorods appear to contain hollow structures, presumably because the nanorods were formed through an aggregation and fusion of smaller adjacent InN nanoparticles.

(19) Yang, C.-M.; Lin, H.-A.; Zibrowius, B.; Spliethoff, B.; Schüth, F.; Liou, S.-C.; Chu, M.-W.; Chen, C.-H. *Chem. Mater.* **2007**, *19*, 3205.

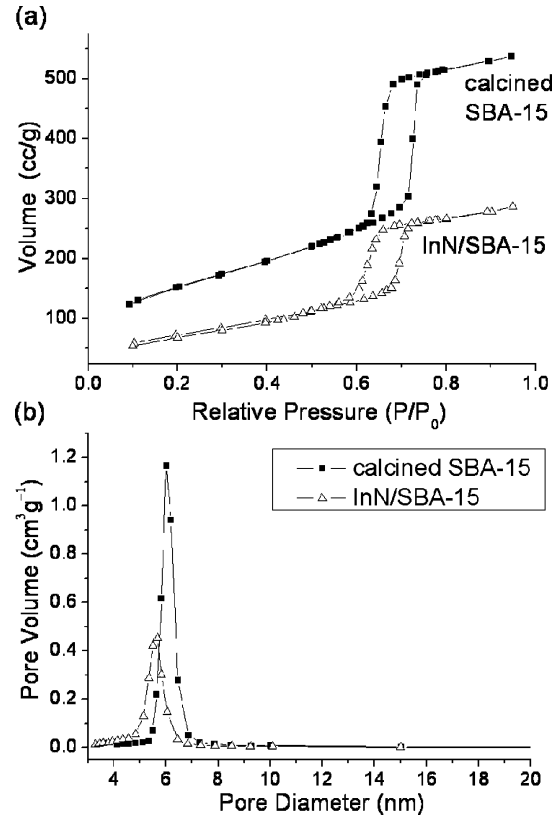

Figure 7. (a) Nitrogen adsorption–desorption isotherms of calcined SBA-15 and InN-incorporated SBA-15. (b) Pore diameter distribution of the samples calculated from the desorption branch of the isotherms using the BJH algorithm.

Table 1. Nitrogen Adsorption–Desorption Isotherm Data[a] and the Wall Thicknesses for the Two SBA-15 Samples

	N adsorption isotherm			wall
sample	S_{BET}/m^2 g^{-1}	V_t/cm^3 g^{-1}	D_{BJH}/nm	thickness/nm
SBA-15	544	0.83	6.0	4.6
InN/SBA-15	272	0.44	5.7	3.8

[a] Legend: S_{BET}, BET specific surface area; V_t, total pore volume; D_{BJH}, pore diameter calculated using the BJH method. The wall thickness is calculated from $A_0 - D_{BJH}$, where $A_0 = (2/3^{1/2})d_{(100)}$.

Figure 6c presents the selected-area electron diffraction (SAED) pattern of the isolated nanorods. The diffraction rings can be indexed to the (100), (002), (101), (102), (110), (103), and (112) planes of hexagonal InN. In addition, some relatively weak rings are also observed and can be indexed to the (222), (400), (431), (440), and (622) planes of cubic In_2O_3 (JCPDF No. 74-1990). The SAED pattern is in agreement with the XRD result, indicating the presence of a trace amount of In_2O_3 along with the InN nanorods. However, we did not find spherical or rodlike In_2O_3 nanoparticles in our high-resolution TEM examination of the samples.

The nitrogen adsorption–desorption isotherms and pore diameter distribution plots for calcined SBA-15 and InN-incorporated SBA-15 are given in Figure 7. Table 1 summarizes the BET surface areas, total pore volumes, pore diameters, and wall thicknesses of these samples. Both isotherms show type IV hysteresis loops, confirming that these samples possess mesoporous structures. After the formation of arrays of InN nanorods, the surface area and

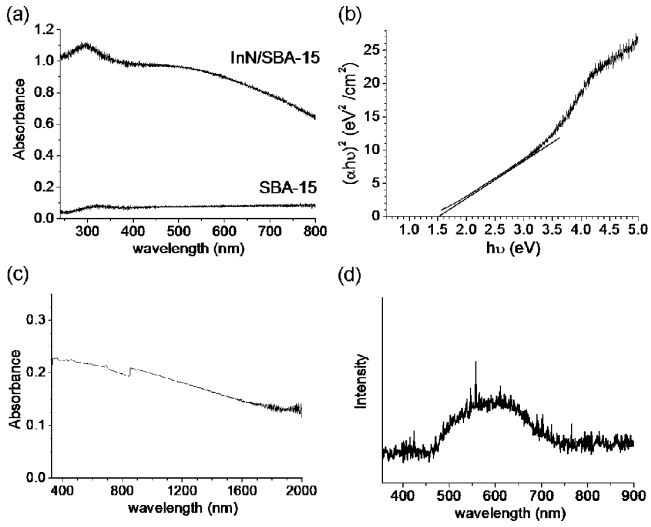

Figure 8. (a) Diffuse reflectance spectrum of calcined SBA-15 and InN-incorporated SBA-15. (b) Plot of $(\alpha h\nu)^2$ vs $h\nu$ for the determination of the direct band gap of the InN nanorods. (c) UV–vis absorption spectrum of the InN nanorods into the near-IR region. The discontinuity in the absorbance at ~850 nm is due to grating/detector change. (d) Photoluminescence spectrum of the InN nanorods within SBA-15 powder using an excitation wavelength of 325 nm from a He−Cd laser.

total pore volume of SBA-15 decrease significantly from 544 to 272 $m^2\ g^{-1}$ and from 0.83 to 0.44 $cm^3\ g^{-1}$, respectively. This suggests high loading of InN nanorods in the mesoporous silica. The pore diameter is around 6 nm. The slight shrinkage in both the pore diameter and wall thickness is attributed to a higher silicate condensation degree after the high-temperature ammonolysis process.

The optical properties of the synthesized InN nanorods have been characterized, and the results are presented in Figure 8. The diffuse reflectance spectrum of the InN-incorporated SBA-15 exhibits a broad band in the visible light region that is centered at around 550–600 nm. This band arises from the absorption of InN nanorods. Another band centered at about 300 nm is attributed to light absorption by a trace amount of In_2O_3 in the sample, which has a wide band gap of 3.67 eV (338 nm) for bulk In_2O_3.[20] The band position is further blue-shifted from the emission maximum of 4 nm In_2O_3 nanoparticles reported at 325 nm, suggesting that the crystallite sizes of In_2O_3 in the InN-incorporated SBA-15 are only a few nanometers.[20] The presence of larger In_2O_3 nanoparticles is also possible. Figure 8b is a plot of $(\alpha h\nu)^2$ vs $h\nu$ for the determination of the direct band gap of the InN nanorods. The band gap of the InN nanorods was found to be around 1.5 eV. This value is believed to be related to the incorporation of oxygen during the nanorod synthesis, as a trace amount of In_2O_3 was also formed. There is no absorption peak in the near-IR region, indicating that the band gap energy of the InN nanorods is not in the near-IR range. Figure 8d gives a photoluminescence spectrum of the InN nanorods confined within SBA-15. A weak and broad peak centered at around 600 nm was recorded. This peak position should also be affected by the incorporation of oxygen in the synthesis of InN nanorods.

(20) Seo, W. S.; Jo, H. H.; Lee, K.; Park, J. T. *Adv. Mater.* **2003**, *15*, 795.

Conclusion

We have demonstrated the first formation of arrays of InN nanorods within the nanoscale channels of mesoporous silica SBA-15. By using $In(NO_3)_3$ as the indium source and methanol as the impregnation medium, silica wall surface functionalization before precursor loading is not needed. Subsequent ammonolysis at 700 °C for 8 h resulted in the formation of InN nanorods with diameters of 6–7.5 nm and lengths of a few tens of nanometers. The formation process and the identity of the InN nanostructures synthesized have been characterized by FT-IR spectra, ^{29}Si MAS NMR spectra, XRD patterns, TEM images, SAED patterns, nitrogen adsorption–desorption isotherm measurements, and optical spectroscopy. A broad absorption band centered at 550–600 nm was observed, and a band gap energy of 1.5 eV was obtained for these InN nanorods. A weak emission band centered at around 600 nm was recorded. These optical properties of the InN nanorods should be related to the incorporation of oxygen during the synthesis. It is expected that the synthetic approach adopted here is extendable to fabricating other rodlike nitride and oxide nanostructures, allowing the examination of novel physical properties.

Acknowledgment. This work was supported by the National Science Council of Taiwan (Grant NSC 95-2113-M-007-031-MY3). We thank Hung-Ying Chen for assistance in the collection of photoluminescence spectra.

Supporting Information Available: Figures giving FT-IR and NMR spectra of calcined SBA-15 powder. This material is available free of charge via the Internet at http://pubs.acs.org.

IC702155W